Absolute Reaction Rate of Chlorine Atoms with Chloroiodomethane

Kyriakos G. Kambanis, Dimitris Y. Argyris, Yannis G. Lazarou,* and Panos Papagiannakopoulos

Department of Chemistry, University of Crete, Heraklion 71409, Crete, Greece

Received: October 27, 1998; In Final Form: February 22, 1999

The reaction of Cl atoms with CH_2ClI was studied in the gas phase with the very low pressure reactor (VLPR) technique over the temperature range 273−363 K. The absolute rate constant was found to be $k_1 = 3.13 \pm 0.27 \times 10^{-11}$ cm^3 molecule^{-1} s^{-1} (2σ uncertainty), independent of temperature. The reaction occurs through iodine atom abstraction leading to CH_2Cl and ICl products. The secondary reaction of Cl atoms with ICl as well as the self-reaction of CH_2Cl radicals was also occurring, leading to the production of I atoms, Cl_2, CH_2═CHCl, and HCl, respectively. Ab initio calculations at the MP2/3-21++G(2d,2p) level of theory suggest that the title reaction may proceed via the intermediate formation of a weakly bound adduct CH_2ClI−Cl, with an I−Cl bond strength of 54.8 kJ mol^{-1}. The enthalpies of formation for CH_2ClI and CHClI at 298.15 K were also calculated at the MP2/3-21++G(2d,2p) level of theory to be 13.0 and 212.0 kJ mol^{-1}, respectively.

Introduction

Chloroiodomethane is among the iodine-containing compounds that have been detected in several geographical regions in the marine ambient air and seawater samples.[1−4] The major sources of CH_2ClI and other iodinated species are the oceanic water masses, with emission rates in the range of ca. 10^6 kg per year.[4] In addition, CH_2ClI may be generated from other iodinated species via halogen-exchange reactions or heterogeneous reactions on sea salt surfaces.[1,5] The dominant degradation pathway of CH_2ClI in the troposphere is expected to be its sunlight photolysis yielding iodine atoms; the atmospheric photodissociation rates[6,7] and photodecomposition dynamics[8] of CH_2ClI have been previously studied. However, there may be additional degradation pathways of CH_2ClI in the troposphere via its reactions with atmospheric species such as OH radicals and Cl atoms, which do not lead directly to iodine atoms production. In particular, the reaction of CH_2ClI with Cl atoms may be important in marine environments, where both concentrations may be sufficiently higher.[9] Therefore, the mechanistic and kinetic study of the title reaction may elucidate the degradation mechanism of CH_2ClI and the fate of iodinated species in the troposphere. The rate constant of this reaction was recently measured by a relative rate technique over the temperature range 206−432 K.[10] The reaction was reported to proceed via iodine atom transfer with a negative activation energy of 1.62 kJ mol^{-1} and a room temperature rate constant of 8.5×10^{-11} cm^3 molecule^{-1} s^{-1}, independent of the N_2 buffer gas pressure in the range 5−700 Torr.

In the present work, we have measured the absolute rate constant of the title reaction in the temperature range 273−363 K, by employing the very low pressure reactor in a modulated molecular flow system.[11] Besides the reaction rate parameters, we were also able to specify the reaction channels of this reaction by mass spectroscopic analysis of the final products. Our technique provides reliable absolute rate constants for fast atom−molecule reactions in the gas phase as well as a clarification of the reaction mechanism by mass spectroscopic analysis of the reaction products.

A number of experimental studies[12,13] and recent theoretical calculations[13,14] have suggested the intermediate formation of weakly bound adducts between chlorine atoms and iodinated compounds. In the present study, a theoretical calculation of the structure and stability of the CH_2ClI−Cl adduct has been performed at the MP2/3-21++G(2d,2p) level of theory, in order to assess the possibility of an adduct formation pathway during the course of the title reaction. The C−H, C−Cl, and C−I bond strengths and the enthalpies of formation for CH_2ClI and CHClI radical, at 298.15 K, were also derived at the MP2/3-21++G(2d,2p) level of theory. Finally, the mechanism and the kinetics for the title reaction were also compared to the corresponding data for the reactions of Cl atoms with the other monohalomethanes, and the effect of pressure on the kinetics of the system was discussed in the context of RRKM theory.

Experimental Section

The reaction of chlorine atoms with chloroiodomethane was studied by using the very low pressure reactor (VLPR) apparatus, whose brief description follows. The reaction takes place in a cylindrical Knudsen type flow reactor connected through a variable exit aperture to the first stage of a differentially pumped system. Thus, reactants and products are continuously escaping the reactor forming an effusive molecular beam that is modulated by a mechanical fork chopper operating at 200 Hz, before it reaches the ionization region of a quadrupole mass spectrometer (Balzers QMG511). The modulated mass spectrometric signal is amplified by a lock-in amplifier (NF model 570), and is further stored on a microcomputer (DEC PDP-11/23) for the subsequent data analysis.

Chlorine atoms were produced by flowing a mixture of 5% Cl_2 in helium (Linde 4.6) through a quartz tube, coated with a thin film of baked phosphoric acid to inhibit Cl atom recombination, and enclosed in a 2.45 GHz microwave cavity operating at 35 W. At these irradiation conditions, a large fraction of Cl_2 dissociates inside the quartz tube and produces Cl atoms, and HCl as a side product, resulting in a large decrease of the mass spectrometric peak at *m*/*e* 70 (Cl_2^+) and the appearance of the peaks at *m*/*e* 35 (Cl^+) and 36 (HCl^+).

Chloroiodomethane had a purity of 97% purity (Aldrich), and

10.1021/jp984193c CCC: $18.00
Published on Web 04/10/1999

it was frequently subjected to several freeze−pump−thaw cycles. A gaseous mixture of 3% CH_2ClI in helium (Linde 4.6) was used throughout the experiments.

The flow rates of all gases were determined by following the pressure drop in a known volume as the gas was flowing through a 1 mm × 20 cm capillary. The mass spectrometric signal intensity I_M was related to the steady-state concentration [M] by the expression: $I_M = \alpha_M F_M = \alpha_M k_{esc,M} V[M]$, where α_M is a mass spectrometric calibration factor, F_M is the flow rate, V is the reactor volume, and $k_{esc,M}$ is the escape constant. The steady-state concentration of chlorine atoms was determined by their mass spectrometric intensity at *m*/*e* 35 and their absolute mass spectrometric calibration factor α_{Cl}. The α_{Cl} factor was frequently determined from the mass balance of chlorine-containing species, inside the quartz tube (in the absence of any other reactant):

$$2\Delta F_{Cl_2} = F_{Cl} + F_{HCl}$$

where ΔF_{Cl_2} is the decrease of the flow of Cl_2 as the microwave discharge was turned on. By considering that the flow F_M of a species M is always equal to the ratio I_M/α_M, the above expression becomes

$$2\Delta I_{Cl_2}/\alpha_{Cl_2} = I_{Cl}/\alpha_{Cl} + I_{HCl}/\alpha_{HCl}$$

where ΔI_{Cl_2} is the intensity drop of the parent peak of Cl_2 at *m*/*e* 70. The absolute calibration factor of Cl_2 was determined from calibration curves of the Cl_2/He mixture, by plotting I_{70} versus F_{Cl_2}. The calibration factor of HCl, α_{HCl}, was determined in separate titration experiments to be a factor of 1.1 ± 0.1 higher than that of α_{Cl}. Thus, the mass spectrometric calibration factor of Cl, α_{Cl}, was calculated from the last expression, by plotting the sum $(1.1I_{Cl} + I_{HCl})$ versus $2.2\Delta I_{Cl_2}/\alpha_{Cl2}$.

The electron ionization energy was kept low at 19 eV in order to suppress the fragmentation of HCl to Cl^+ (*m*/*e* 35) down to negligible levels (less than 0.3%). At this electron energy, the mass spectrum of chloroiodomethane shows the peaks (*m*/*e*, relative intensities): 49 (100), 51 (30), 141 (1), 176 (3), and 178 (1), which correspond to the ions $CH_2{}^{35}Cl^+$, $CH_2{}^{37}Cl^+$, CH_2I^+, $CH_2{}^{35}ClI^+$, and $CH_2{}^{37}ClI^+$ respectively. Both fragment peaks at *m*/*e* 49 and 176 were used to monitor the steady-state concentration of chloroiodomethane. However, the mass spectrometric interference of chloromethyl radical product CH_2Cl in the intensity of peak at *m*/*e* 49 ($CH_2{}^{35}Cl^+$) is unlikely, considering that halogenated radicals undergo complete fragmentation at an electron energy of 19 eV, and thus they lack a mass spectrometric parent peak. Indeed, the kinetic results obtained by using either peak did not show any systematic variation, therefore the more intense peak of CH_2ClI at *m*/*e* 49 was employed for the kinetic analysis. The mass spectrometric sensitivity factor α_{CH_2ClI} was determined by calibration plots of the intensity I_{49} versus F_{CH_2ClI}. The initial concentration of Cl atoms was in the range $(0.3-1.5) \times 10^{12}$ molecules cm^{-3}, and the initial concentration of CH_2ClI was in the range $(0.1-3.3) \times 10^{12}$ molecules cm^{-3}. The uncertainty of the mass spectral intensity measurements was ca. 3%, and thus the ratio $R = [CH_2ClI]_0/[CH_2ClI] = I_{CH_2ClI,0}/I_{CH_2ClI}$ was determined with an accuracy of ca. 5% (2σ).

The reactor ($V = 168$ cm^3) was coated with a thin film of Teflon in order to inhibit wall reactions, and its temperature was controlled by circulating a thermostated liquid through the outer jacket. The escape constants of various species were determined by monitoring the first-order decay of their mass spectrometric signal after a fast halt of the flow. The escape aperture had a diameter of 5 mm and the escape constants of various species were given by the expression $k_{esc,M} = 1.86\text{-}(T/M)^{1/2}$ s^{-1}, where T is the reactor temperature and M is the molecular mass of the escaping species. The total pressure inside the reactor was in the range 0.6−1.5 mTorr.

Results

The reaction of atomic chlorine with chloroiodomethane may proceed via the following primary reaction channels:

$$Cl + CH_2ClI \rightarrow HCl + CHClI \qquad \Delta H^\circ_r = -14.2 \pm 15 \tag{1a}$$

$$\rightarrow ICl + CH_2Cl \qquad \Delta H^\circ_r = +5.0 \pm 15 \tag{1b}$$

$$\rightarrow I + CH_2Cl_2 \qquad \Delta H^\circ_r = -122.6 \pm 15 \tag{1c}$$

The reaction enthalpies ΔH°_r at 298.15 K were derived by using the experimental enthalpies of formation ΔH°_f available for all species,[15,16] with the exception of CH_2ClI and CHClI whose formation enthalpies were theoretically calculated, as described below. By using the theoretical values of ΔH°_f for CH_2Cl and CH_2Cl_2, the corresponding reaction enthalpies for channels 1b and 1c were calculated to be higher, 15.5 and −116.0 kJ mol^{-1}, respectively. However, the former values are considered more reliable, by taking into account the higher estimated uncertainty (>10 kJ mol^{-1}) of the formation enthalpies theoretically calculated.

The most probable secondary reactions are

$$Cl + ICl \rightarrow Cl_2 + I \tag{2}$$

$$Cl + CH_2Cl \rightarrow CH_2Cl_2 \tag{3}$$

$$Cl_2 + CH_2Cl \rightarrow CH_2Cl_2 + Cl \tag{4}$$

$$CH_2Cl + CH_2Cl \rightarrow CH_2{=}CHCl + HCl \tag{5}$$

The mass spectrometric analysis of the reaction products revealed the appearance of three new peaks at *m*/*e* 62 ($C_2H_3Cl^+$), 127 (I^+), and 162 (ICl^+), and an increase of the peaks at 36 (HCl^+) and 70 (Cl_2^+). The peaks at *m*/*e* 36 and 162 correspond to HCl and ICl products, while the peaks at *m*/*e* 62, 70, and 127 correspond to the secondary products $CH_2{=}CHCl$, Cl_2, and I atoms, respectively. There was no mass spectroscopic evidence of CH_2Cl_2 product at *m*/*e* 84 ($CH_2{}^{35}Cl_2^+$), which suggested the absence of primary reaction 1c and secondary reactions 3 and 4. Reaction 1c is expected to have a low rate constant since it proceeds through a fairly tight transition state with a five-coordinated carbon atom. The termolecular recombination reaction 3 was very unlikely to occur in our very low-pressure conditions. Reaction 4 has a low rate constant $k_4 = 3.10 \times 10^{-13}$ cm^3 $molecule^{-1}$ s^{-1},[17] and therefore its participation in the reaction scheme should be negligible. The appearance of Cl_2 molecules and I atoms among the reaction products indicates the presence of secondary reactions 2 and 5. The presence of these reactions is due to their high rate constants, $k_2 = 1 \times 10^{-11}$ and $k_5 = 2.9 \times 10^{-11}$ cm^3 $molecule^{-1}$ s^{-1},[19] respectively.

Application of the steady-state approximation for the species Cl, CH_2ICl, ICl, and Cl_2 results in the following expressions ($\Delta[Cl]$, $\Delta[CH_2ClI]$ are used to denote the steady-state concentration difference with the addition of CH_2ICl or Cl, respectively. $\Delta[Cl_2]$ denotes the steady-state concentration difference of Cl_2, with the addition of CH_2ICl reactant):

$$\Delta[\mathrm{Cl}]k_{\mathrm{esc,Cl}} = k_1[\mathrm{Cl}][\mathrm{CH_2ClI}] + k_2[\mathrm{Cl}][\mathrm{ICl}] \quad \text{(I)}$$

$$\Delta[\mathrm{CH_2ClI}]k_{\mathrm{esc,CH_2ClI}} = k_1[\mathrm{Cl}][\mathrm{CH_2ClI}] \quad \text{(II)}$$

$$[\mathrm{ICl}]k_{\mathrm{esc,ICl}} = k_{1b}[\mathrm{Cl}][\mathrm{CH_2ClI}] - k_2[\mathrm{Cl}][\mathrm{ICl}] \quad \text{(III)}$$

$$\Delta[\mathrm{Cl_2}]k_{\mathrm{esc,Cl_2}} = k_2[\mathrm{Cl}][\mathrm{ICl}] \quad \text{(IV)}$$

After rearrangement, expression (II) becomes

$$(R-1)k_{\mathrm{esc,CH_2ICl}} = k_1[\mathrm{Cl}] \quad \text{(V)}$$

where $R = [\mathrm{CH_2ClI}]_0/[\mathrm{CH_2ClI}] = I_{\mathrm{CH_2ClI,0}}/I_{\mathrm{CH_2ClI}}$ (subscript 0 denotes the absence of reactant Cl). Expression V, without complications from secondary reactions, was used for the determination of the rate constant k_1, and a typical plot at 303 K is presented in Figure 1. The linear least-squares fits to the data yield the rate constant k_1 with a precision of ca. 5% (2σ).

Experiments were performed at 273, 303, 333, and 363 K, and the initial reactant concentrations as well as the rate constants obtained are listed in Table 1. The corresponding Arrhenius plot, including the results of the previous study,[10] is presented in Figure 2. Linear least-squares fit of the temperature dependence data yields the activation energy and the preexponential A factor for reaction 1, leading to a rate constant k_1 expressed as (2σ uncertainty):

$$k_1 = (3.19 \pm 0.13) \times 10^{-11} \times \exp[(-7.0 \pm 22.9)/T]\ \mathrm{cm^3\ molecule^{-1}\ s^{-1}}$$

Therefore, the rate constant of the title reaction can be considered to be temperature independent in the temperature range 273−363 K, and the average value of k_1 is $(3.13 \pm 0.27) \times 10^{-11}$ cm^3 molecule^{-1} s^{-1} (2σ uncertainty).

By solving expression IV for [ICl], and substituting in expression III, the following expression is obtained:

$$(\Delta[\mathrm{Cl_2}]k_{\mathrm{esc,Cl_2}}/[\mathrm{Cl}])(1 + k_{\mathrm{esc,ICl}}/k_2[\mathrm{Cl}]) = k_{1b}[\mathrm{CH_2ICl}] \quad \text{(VI)}$$

By taking into account that the rate constant k_2 between ICl molecules and Cl atoms has been measured to be 1.0×10^{-11} cm^3 molecule^{-1} s^{-1} at 298 K,[18] a plot of expression VI provides the rate constant k_{1b}, as shown in Figure 3 at the temperature of 303 K. Linear least-squares fit of the data yields the rate constant for I atom metathesis, $k_{1b} = (3.26 \pm 0.18) \times 10^{-11}$ cm^3 molecule^{-1} s^{-1} (2σ). The rate constant k_{1b} derived is slightly higher than the overall k_1 rate constant at 303 K, and this may be due to either the underestimation of the rate constant k_2 or the propagation of small experimental errors in plotting expression VI. Nevertheless, the near equality of k_{1b} to the overall rate constant k_1 suggests that the title reaction is occurring exclusively via I atom metathesis, reaction 1b, leading to ICl and CH_2Cl products.

Theoretical Calculation of the Thermochemistry of CH_2ClI, CHClI Radical, and $CH_2ClI-Cl$ Adduct. Ab initio theoretical calculations on the structure and energetics of the various iodinated species of this study were performed by using the GAMESS programs package.[20] The 3-21G basis set was employed, augmented by two sets of polarization functions on d and p orbitals, with the addition of diffuse functions on s and p orbitals, on all atoms. Restricted Hartree−Fock wave functions (RHF-SCF) were used for all closed-shell species and unrestricted Hartree−Fock wave functions (UHF-SCF) were used for all radical species. Electron correlation of the valence electrons was taken into account by second-order Møller−Plesset perturbation theory (MP2, frozen core). The geometries and the vibrational frequencies of all closed-shell iodinated species were calculated at the MP2/3-21++G(2d,2p) level of theory by the method of analytical gradients, while the geometry of the open-shell $CH_2ClI-Cl$ adduct was optimized by a nongradient optimization method. The geometry optimization and vibrational frequencies calculation for all other radical species were performed at the UHF/3-21++G(2d,2p) level of theory (without electron correlation). The geometry optimization and the vibrational frequencies calculation of CH_4 were performed at the 6-311++G(2d,2p) level of theory, followed by single-point energy calculation at the MP2/3-21++G(2d,-2p) level. All vibrational frequencies were scaled down by the factor 0.89, in order to take anharmonicity effects into account.[21] Finally, the total enthalpy of every species was calculated at 298.15 K, by assuming the rigid-rotor and harmonic oscillator

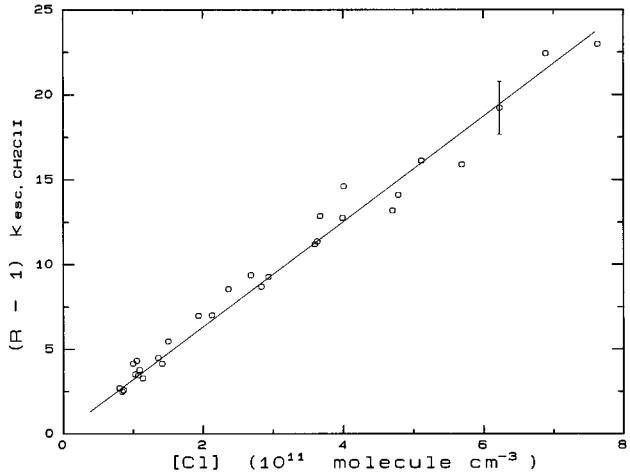

Figure 1. Plot of $(R-1)k_{\mathrm{esc,CH_2ClI}}$ versus [Cl] at 303 K. Error bar reflects the propagated errors (2σ).

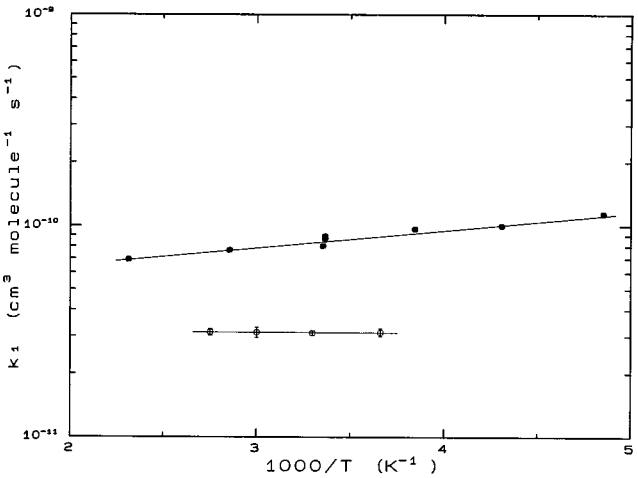

Figure 2. Arrhenius plot of k_1 versus 1000/T. Error bars reflect the total propagated errors (2σ) (open circles, this study; filled circles, data from ref 10).

TABLE 1: Initial Concentrations of Cl and CH_2ClI Reactants and Reaction Rate Constants k_1 (in 10^{-11} cm^3 Molecule^{-1} s^{-1}) at Temperatures of 273, 303, 333, and 363 K

T (K)	$[\mathrm{Cl}]_0$ (10^{11} molecules cm^{-3})	$[\mathrm{CH_2ClI}]_0$ (10^{11} molecules cm^{-3})	no. of points	$k_1 \pm 2\sigma$
273	4.8−10.0	2.2−30.2	39	3.13 ± 0.14
303	4.9−9.0	1.2−28.6	30	3.11 ± 0.08
333	3.6−7.5	1.6−30.7	34	3.13 ± 0.18
363	2.7−14.4	1.1−32.3	47	3.14 ± 0.12

TABLE 2: Theoretically Determined Geometries (Bond Lengths in Å, Angles in deg), Vibrational Frequencies (in cm^{-1}), Total Electronic Energies (in hartrees, 1 hartree = 2625.5 kJ mol^{-1}), and Total Enthalpies (at T = 298.15 K) for All Species Involved in the Calculations, at the MP2/3-21++G(2d,2p) Level of Theory

species	structural parameters	vibrational frequencies	total energy	total enthalpy at 298.15 K
H			−0.497 800	−0.495 440
Cl			−457.477 738	−457.475 378
I			−6888.123 327	−6888.120 967
CH_4	r(C−H) = 1.087 ∠H−C−H = 109.47	1376.15, 1377.20 (2), 1573.78 (2), 3108.55, 3231.01, 3247.97, 3254.75	−40.143 784	−40.099 152
CH_3Cl	r(C−H) = 1.084 r(C−Cl) = 1.830 ∠Cl−C−H = 107.38	703.03, 1035.72, 1036.18, 1402.06, 1497.23, 1498.21, 3169.72, 3287.20, 3304.97	−497.081 959	−497.043 568
CH_3I	r(C−H) = 1.083 r(C−I) = 2.199 ∠I−C−H = 107.29	530.27, 911.68, 912.61, 1326.44, 1482.66, 1483.78, 3170.35, 3292.53, 3311.99	−6927.692 323	−6927.654 814
CH_2ClI	r(C−H) = 1.080 r(C−Cl) = 1.806 r(C−I) = 2.192 ∠I−C−Cl = 112.65 ∠I−C−H = 107.64 ∠I−C(−Cl)−H = 119.16 ∠H−C(−Cl)−H = 121.68	191.44, 534.29, 711.40, 791.78, 1160.69, 1242.73, 1440.98, 3236.78, 3337.75	−7384.627 680	−7384.597 086
CH_2Cl	r(C−H) = 1.069 r(C−Cl) = 1.731 ∠Cl−C−H = 117.21 ∠Cl−C−(H)−H= 181.01	150.83, 811.85, 1049.29, 1498.77, 3356.15, 3533.01	−496.414 906	−496.390 188
CH_2I	r(C−H) = 1.070 r(C−I) = 2.097 ∠Cl−C−H = 118.55 ∠Cl−C−(H)−H = 179.98	304.52, 607.73, 894.25, 1449.52, 3350.69, 3518.78	−6927.022 449	−6926.997 397
CHClI	r(C−H) = 1.069 r(C−Cl) = 1.722 r(C−I) = 2.093 ∠I−C−Cl = 121.45 ∠Cl−C−H = 120.02 ∠I−C−(Cl)−H = 164.42	211.29, 242.66, 577.28, 868.30, 1272.18, 3457.26	−7383.961 483	−7383.942 827
CH_2ClI−Cl adduct	r(C−H) = 1.080 r(C−Cl) = 1.797 r(C−I) = 2.199 r(I−Cl) = 2.738 ∠I−C−Cl = 111.67 ∠I−C−H = 106.50 ∠I−C(−Cl)−H = 117.29 ∠H−C(−Cl)−H = 120.32 ∠Cl−I(−C)−Cl = 179.53	98.96, 162.55, 192.50, 214.27, 547.39, 738.56, 907.46, 1247.98, 1321.51, 1546.45, 3286.47, 3396.80	−7842.127 902	−7842.093 343

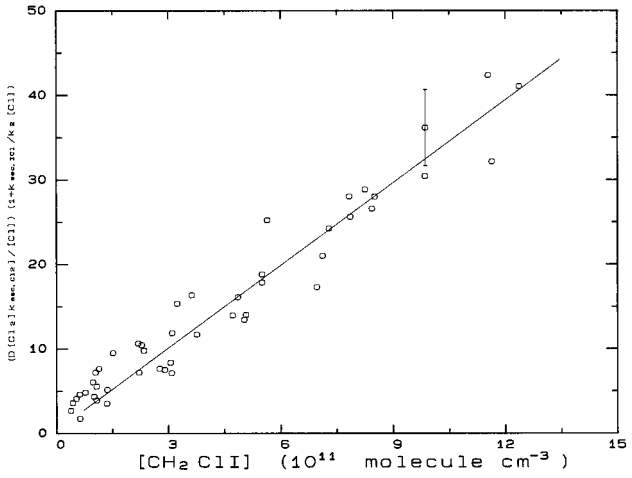

Figure 3. Plot of $(\Delta[Cl_2]k_{esc,Cl_2}/[Cl])(1 + k_{esc,ICl}/k_2[Cl])$ versus $[CH_2ICl]$ at T = 303 K. k_2 was taken to be 1.0×10^{-11} cm^3 $molecule^{-1}$ s^{-1}, from ref 18. Error bar reflects the propagated errors (2σ).

approximations. The optimized geometries, vibrational frequencies, total electronic energies, and total enthalpies calculated for all species are displayed in Table 2.

The enthalpy of formation $\Delta H°_f$ of CH_2ClI at 298.15 K was obtained by using the theoretical enthalpy difference of the isodesmic reaction

$$CH_3I + CH_3Cl \rightarrow CH_2ClI + CH_4$$

combined with the experimental enthalpies of formation of CH_3I (+14.6 kJ mol^{-1}), CH_3Cl (−82.0 kJ mol^{-1}), and CH_4 (−74.8 kJ mol^{-1}).[16] The enthalpy of formation derived for CH_2ClI was +13.0 kJ mol^{-1}, which is very close to +13.4 kJ mol^{-1}, the average of the corresponding experimental values for CH_2Cl_2 (−95.4 kJ mol^{-1}) and CH_2I_2 (+122.2 kJ mol^{-1}).[15,16] The enthalpy of formation of CH_2Cl_2 was similarly calculated by the isodesmic reaction

$$CH_3Cl + CH_3Cl \rightarrow CH_2Cl_2 + CH_4$$

to be −88.8 kJ mol^{-1}, higher by 6.6 kJ mol^{-1} than the currently accepted value.[16]

The C−X (X = H, Cl, I) bond enthalpies for CH_2ClI were calculated to be 417.0, 326.4, and 225.6 kJ mol^{-1}, respectively. Furthermore, by considering the experimental enthalpies of formation for the H, Cl and I atoms,[16] the enthalpies of formation for the CHClI, CH_2I, and CH_2Cl radicals were calculated to be 212.0, 218.5, and 131.9 kJ mol^{-1}, respectively. The corresponding experimental values reported for CH_2I and CH_2Cl radicals are 217.6 and 121.3 kJ mol^{-1},[16] which are in good agreement

TABLE 3: Room Temperature Rate Constants, Preexponential *A* Factors, Activation Energies, and Reaction Enthalpies for Hydrogen/Halogen Metathesis Reactions of Chlorine Atoms with Methane and Halogenated Methanes

species	$k_{298} \times 10^{13}$ (cm^3 molecule^{-1} s^{-1})	$A \times 10^{11}$ (cm^3 molecule^{-1} s^{-1})	E_a (kJ mol^{-1})	ΔH_r(HCl/XCl) (kJ mol^{-1})	ref
CH_4	1.03	1.10	11.7	+8.03	16
CH_3F	3.5	2.0	10.0	−12.4/+209.2	16
CH_3Cl	4.8	3.2	10.4	−9.9/+107.5	16
CH_3Br	4.83	1.66	8.9	−10.3/+77.7	22
CH_3I	13.7	1.33	5.7	−10.3/+28.5	23
CH_2ClI	311	3.13	0	−14.2/+5.0	this work
	805	4.4	−1.6		10

with our calculated values. A comparison of the experimentally available values with our theoretical estimates shows that the C−Cl and C−I bond enthapies calculated for CH_2ClI are both lower that the experimental ones for CH_3Cl (349.4 kJ mol^{-1}) and CH_3I (238.6 kJ mol^{-1}), the latter inferred from the formation enthalpies reported for the relevant species.[16] Therefore, the results are consistent with the general trend of carbon−halogen bonds weakening by increasing substitution in methyl halides. The calculated CHClI−H bond enthalpy is lower by ca. 4 kJ mol^{-1} than the experimental C−H bond enthalpies for CH_3Cl (420.9 kJ mol^{-1}) and CH_3I (421.3 kJ mol^{-1}). The above results indicate that the presently employed theoretical method constitutes a reliable tool for the calculation of thermochemical quantities of iodinated compounds.

The general features of the theoretically determined structure of the CH_2ClI−Cl adduct resemble those of the previously studied adducts CH_3I−Cl and CH_3OCH_2I−Cl.[13,14] More specifically, it possesses a relatively long I−Cl bond of 2.738 Å and a fairly close C−I−Cl angle of 76.21°. The Cl atom is directed away from the other Cl atom connected to the carbon atom, probably due to nonbonding electron repulsions, and the overall geometry of the parent halide is slightly altered upon chlorine atom attachment. The CH_2ClI−Cl bond enthalpy has been calculated to be 54.8 kJ mol^{-1}, at the MP2/3-21++G(2d,2p) level of theory, slightly higher than the values 52.4 and 51.3 kJ mol^{-1} for CH_3I−Cl and CH_3OCH_2I−Cl adducts, calculated at the same level of theory.[14] A value of 79.1 kJ mol^{-1} was derived for the enthalpy of formation for the adduct, by using the experimental enthalpy of formation for Cl atom (120.9 kJ mol^{-1}), and the theoretical value for CH_2ClI, calculated in the present study.

Discussion

Our results indicate that the title reaction proceeds exclusively via the abstraction of an iodine atom and results in the formation of ICl, which is in agreement with the results of previous work.[10] However, the value of the rate constant at low pressures (0.6−1.5 mTorr of He) is ca. 2.5 times slower than its value at much higher pressures (5−700 Torr of N_2). The preexponential factors are slightly closer, while the low-pressure rate constant shows no temperature dependence, in contrast with the small negative activation energy of the reaction conducted at high pressures. Therefore, the kinetics of the title reaction possibly shows a pressure dependence, as in the reaction of C_2H_5 radical with O_2[24] which involves the formation of a relatively stable radical intermediate.

The rate parameters of the title reaction can be compared with the corresponding parameters for the reactions of Cl atoms with CH_4, CH_3F, CH_3Cl, CH_3Br, and CH_3I,[16,22,23] listed in Table 3. The reaction rate of Cl atoms with CH_2ClI is much faster than those with monohalomethanes, which proceed predominantly via hydrogen atom transfer. The exothermicity of the hydrogen transfer reactions tends to increase with the size of the halogen atom, followed by a remarkable decrease of the activation energy. Thus, despite the small counteracting decline of the preexponential factors, the corresponding rate constants are monotonically increasing. However, the abrupt decrease of the activation energies does not follow the corresponding trend of exothermicity and suggests the intermediate formation of an adduct RX−Cl (X = Br, I), whose stability depends on the polarizability and the electron-donating ability of the halogen atom. Indeed, on the basis of the calculated X−Cl bond strengths, the adduct-forming pathway is likely to be more important for the iodine-containing molecules.[13,14,22,25] In the reactions of monohalomethanes with Cl atoms, halogen atom metathesis was not observed (with the exception of the reaction of CH_3I with Cl atoms, in molecular beams, at high relative translational energies[12]) and this result can be explained considering the high endothermicity of this pathway, as shown in Table 3. Thus, the hydrogen transfer remains the only energetically accessible forward pathway, and at ordinary temperatures the reactions lead exclusively to HCl and the corresponding halomethyl radical.

In the reaction of Cl with CH_2ClI, the calculations suggest that the iodine transfer pathway is mildly endothermic by 5.0 kJ mol^{-1} (a value subject to a rather high uncertainty), while the hydrogen transfer pathway is exothermic by 14.2 kJ mol^{-1}, and therefore the iodine transfer pathway becomes thermochemically more accessible. Due to the long-range attractive interactions of the chlorine atom with the iodine atom,[14] the encounter of a Cl atom with a CH_2ClI molecule may proceed to the formation of a CH_2ClI−Cl adduct, which may be collisionally deactivated. The unimolecular decomposition of the adduct, besides its dissociation back to reactants, may follow two different forward pathways, either the thermochemically favored four-center elimination of HCl, which is entropically unlikely, or, the elimination of ICl, which proceeds through an entropically favored transition state. Furthermore, due to the extensive molecular rearrangements required, a relatively high potential barrier may be associated with the HCl elimination pathway, allowing the ICl dissociation pathway to dominate, as suggested by the analysis of the reaction products.

The overall reaction (including the collisional deactivation pathway) can be described by the following scheme:

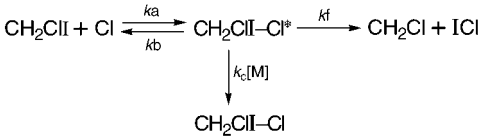

Application of the steady-state approximation leads to the following expression for the overall rate constant k_{obs} of the reactants disappearance:

$$k_{obs} = k_a\{1 - \{k_b/(k_b + k_f + k_c[M])\}\} = k_a\{1 - \{\beta/(1 + \beta + k_c[M]/k_f)\}\} \quad \text{(VII)}$$

where $\beta = k_b/k_f$.

In the low-pressure regime, the contribution of the collisional term $k_c[M]$ is negligible, and thus the energized adduct cannot be effectively stabilized by collisions and follows either the route back to reactants via a transition state TS_b or the forward direction to products via a transition state TS_f. In the context of the RRKM theory,[26] the ratio $\beta = k_b/k_f$ of the corresponding rate constants is equal to the ratio W_b/W_f of the sums W of the quantum states for the active degrees of freedom for the corresponding transition states. The low frequency of deenergizing collisions allows a nonthermal energy distribution for the newly formed adduct and the ratio $\beta = W_b/W_f$ of the large sums of states at these relatively high energies should vary little with energy, leading to a weak dependence of β on temperature. Therefore, by assuming that k_a approaches the gas-kinetic collision rate coefficient (possessing a small dependence on $T^{1/2}$), the activation energy should also be small (either negative or positive) for the reaction conducted in the low-pressure regime.

At the high end of the pressure range, the energy-rich $CH_2ClI-Cl^*$ adduct is collisionally stabilized (an effect similar to that observed for the $CH_2ClBr-F$ adduct[27]), resulting in an increase of the rate constant for the disappearance of Cl atoms, in accordance with the results of the previous study.[10] In addition, the energy distribution among the various degrees of freedom for the adduct approaches the thermal one, and hence, the temperature dependence of the reaction at high pressures should be very sensitive to the dependence of β on the energy quite close to the potential energy barriers. Theoretical calculations have shown the absence of a entrance potential energy barrier for the Cl atom attachment on CH_3I and CH_3OCH_2I,[14] as would be also expected for CH_2ClI. Therefore, V_b is probably zero, and V_f is at least equal to the reaction endothermicity. Since the forward pathway involves greater molecular rearrangements, its associated transition state TS_f could be considered tighter than TS_b. Therefore, at energies above the potential energy thresholds, the sum of states W function rises steeper for the more loose TS_b (considering also that $V_b < V_f$), and given a statistical Maxwell−Boltzmann energy distribution for the adduct, β increases with temperature, resulting in a negative activation energy for the overall reaction. This simplified picture accounts for the variation in the kinetic behavior of the reaction system from a low- to the high-pressure limit, as the result of the gradual collisional stabilization and thermalization of the intermediate adduct.

The mechanism and the rate constant of the title reaction may be compared with the corresponding one for the reaction of Cl atoms with CH_3I. In the latter, the intermediate formation of a similar adduct has also been experimentally[12,13] and theoretically[13,14] proposed. In the case of the CH_3I-Cl adduct, the C−I bond fission process is significantly endothermic, and the only accessible forward pathway is that of HCl elimination. Therefore, the pathway of dissociation back to reactants competes effectively with the forward pathway of decomposition to CH_2I and HCl products, considering the energetic and entropic impediments associated with the four-center HCl elimination. In contrast, for the $CH_2ClI-Cl$ adduct, the entropically favored pathway of decomposition to CH_2Cl and ICl products is more competitive, since the C−I bond energy is weaker, resulting in a rate constant higher by more than an order of magnitude.

The rather fast reaction rate of Cl atoms with CH_2ClI suggests that this reaction may play a primary role in the removal of CH_2ClI molecules from the troposphere and results in the formation of ICl molecules, in agreement with the conclusions of the previous work.[10] It should be pointed out that this degradation pathway of CH_2ClI does not lead to iodine atoms but to relatively stable ICl molecules, implying the contribution of a different iodine cycle in the marine boundary layer. The lifetime of ICl is determined probably by its sunlight photodissociation to iodine and chlorine atoms. Another possible degradation process of ICl may be carried over by its hydrolysis to hypoiodous acid, IOH, which is finally dissolved in seawater.

References and Notes

(1) Class, T. H.; Ballschmiter, K. *J. Atm. Chem.* **1988**, *6*, 35−46.
(2) Reifenhauser, W.; Heumann, K. G. *Atmos. Environ.* **1992**, *26*(*A*), 2905−2912.
(3) Schall, C.; Heumann, K. G. *Fresenius J. Anal. Chem.* **1993**, *346*, 717−722.
(4) Yokouchi, Y.; Barrie, L. A.; Toom, D.; Akimoto, H. *Atm. Environ.* **1996**, *30*, 1723−1727.
(5) Moore, R. M.; Tokarczyk, *J. Geophys. Res.* **1992**, *19*, 1779.
(6) Rattigan, O. V.; Shallcross, D. E.; Cox, R. A. *J. Chem. Soc., Faraday Trans.* **1997**, *93*, 2839.
(7) Roel, C. M.; Burkholder, J. B.; Moortgat, G. K.; Ravishankara, A. R.; Crutzen, P. J. *J. Geophys. Res.* **1997**, *102*, 12819.
(8) Schmitt, G.; Comes, F. J. *J. Photochem. Photobiol. A* **1987**, *41*, 13−30.
(9) Rudolph, J.; Koppmann, R.; Plass-Dülmer, C. *Atmos. Environ.* **1996**, *30*, 1887−1894.
(10) Bilde, M.; Sehested, J.; Nielsen, O. J.; Wallington, T. J.; Meagher, R. J.; McIntosh, M. E.; Piety, C. A.; Nicovich, J. M.; Wine, P. H. *J. Phys. Chem.* **1997**, *101*, 8035−8041.
(11) Lazarou, Y. G.; Michael, C.; Papagiannakopoulos, P. *J. Phys. Chem.* **1992**, *96*, 1705−1708.
(12) Grice, R. Int. Rev. Phys. Chem. **1995**, *14*, 315.
(13) Ayhens, Y. V.; Nicovich, J. M.; McKee, M. L.; Wine, P. H. *J. Phys. Chem. A* **1997**, *101*, 9382−9390.
(14) Lazarou, Y. G.; Kambanis, K. G.; Papagiannakopoulos, P. *Chem. Phys. Lett.* **1997**, *271*, 280−286.
(15) Benson, S. W. *Thermochemical Kinetics*, 2nd ed.; Wiley-Interscience: New York, 1976.
(16) DeMore, W. B.; Sander, S. P.; Golden, D. M.; Hampson, R. F.; Kurylo, M. J.; Howard, C. J.; Ravishankara, A. R.; Kolb, C. E.; Molina, M. J. "Chemical Kinetics and Photochemical Data for Use in Stratospheric Modelling", *JPL Publication 97−4*, 1997.
(17) Seetula, J. A.; Gutman, D.; Lightfoot, P. D.; Rayes, M. T.; Senkan, S. M. *J. Phys. Chem.* **1991**, *95*, 10688−10693.
(18) Chesnokov, E. N., *Khim. Fiz.* **1991**, 10, 204.
(19) Russel, P. B.; Lightfoot, P. D.; Caralp, F.; Calone, V.; Lesclaux, R.; Forst, W. *J. Chem. Soc., Faraday Trans.* **1991**, *87*, 2367.
(20) Schmidt, M. W., Baldridge, K. K.; Boatz, J. A.; Elbert, S. T.; Gordon, M. S.; Jensen, J. H.; Koseki, S.; Matsunaga, N.; Nguyen, K. A.; Su, S. J.; Windus, T. L.; Dupuis, M.; Montgomery, J. A. *J. Comput. Chem.* **1993**, *14*, 1347−1363.
(21) Hehre, W. J.; Radom, L.; Schleyer, P.v. R.; Pople, J. A. *Ab initio Molecular Orbital Theory*; Wiley-Interscience: New York, 1986.
(22) Kambanis, K. G.; Lazarou, Y. G.; Papagiannakopoulos, P. *J. Phys. Chem.* **1997**, *101*, 8496−8502.
(23) Kambanis, K. G.; Lazarou, Y. G.; Papagiannakopoulos, P. *Chem. Phys. Lett.* **1997**, *268*, 498−504.
(24) Kaiser, E. W.; Rimai, L.; Wallington, T. J. *J. Phys. Chem.* **1989**, *93*, 4094−4098.
(25) Piety, C. A.; Soller, R.; Nicovich, J. M.; McKee, M. L.; Wine, P. H. *Chem. Phys.* **1998**, *231*, 155−169.
(26) Robinson, P. J.; Holbrook, K. A. *Unimolecular Reactions*, Wiley-Interscience: New York, 1971.
(27) Bilde, M.; Sehested, J.; Nielsen, O. J.; Wallington, T. J. *J. Phys. Chem. A* **1997**, *101*, 5477−5488.